Recessive Mutations in VPS13D Cause Childhood Onset **Movement Disorders**

Julie Gauthier, MSc, PhD, 1 Inge A. Meijer, MD, PhD,² Davor Lessel, MD ⁽¹⁾ Niccolò E. Mencacci, MD, PhD,⁴ Dimitri Krainc, MD, PhD,⁴ Maja Hempel, MD,³ Konstantinos Tsiakas, MD.⁵ Holger Prokisch, PhD,^{6,7} Elsa Rossignol, MD, MSc,² Margaret H. Helm, MSc, CGC,8 Lance H. Rodan, MD,⁹ Jason Karamchandani, MD, ¹⁰ Miryam Carecchio, MD, PhD, 11 Steven J. Lubbe, MSc, PhD,⁴ Aida Telegrafi, MS, CGC, 12 Lindsay B. Henderson, PhD, FACMG, 12 Kerry Lorenzo, MSc, CGC, 13 Stephanie E. Wallace, MD, 14 Ian A. Glass, MD, MB ChB, 14 Fadi F. Hamdan, MSc, PhD, 1 Jacques L. Michaud, MD, 15 Guy A. Rouleau, MD, PhD, 16 and Philippe M. Campeau, MD 15

VPS13 protein family members VPS13A through VPS13C have been associated with various recessive movement disorders. We describe the first disease association of rare recessive VPS13D variants including frameshift, missense, and partial duplication mutations with a novel complex, hyperkinetic neurological disorder. The clinical features include developmental delay, a childhood onset movement disorder (chorea, dystonia, or tremor), and progressive spastic ataxia or paraparesis. Characteristic brain magnetic resonance imaging shows basal ganglia or diffuse white matter T2 hyperintensities as seen in Leigh syndrome and choreoacanthocytosis. Muscle biopsy in 1 case showed mitochondrial aggregates and lipidosis, suggesting mitochondrial dysfunction. These findings underline the importance of the VPS13 complex in neurological diseases and a possible role in mitochondrial function.

ANN NEUROL 2018;00:000-000

ovement disorders comprise a wide group of neurological diseases with highly variable, often complex clinical presentation. Classically, they can be subdivided into 2 main phenomenological categories: (1) hyperkinetic disorders including dystonia, chorea, tremor, and myoclonus; and (2) hypokinetic movements such as bradykinesia in parkinsonism. The pathophysiology of movement disorders is still not entirely understood, but most abnormal movements are associated with dysfunction of the basal ganglia or their interconnected brain regions such as the thalamus, cerebellum, and sensorimotor cortex. Although causative mutations in >200 genes have been associated with various movement disorders, many patients remain without a precise genetic diagnosis. Here, we report mutations in VPS13D as a novel cause of spastic ataxia, chorea, and dystonia in 5 unrelated families.

VPS13D is part of the VPS13 family of ubiquitously expressed genes encoding 4 proteins highly conserved in eukaryotic cells (VPS13A-D).^{2,3} Recently Vps13D has been shown to play an important role in mitochondrial size, autophagy, and clearance.4 Genetic

From the ¹Molecular Diagnostic Laboratory and Division of Medical Genetics, Department of Pediatrics, Saint Justine University Hospital Center, Montreal, Canada; ²Department of Neuroscience, University of Montreal, Montreal, Canada; ³Institute of Human Genetics, University Medical Center Hamburg-Eppendorf, Hamburg, Germany; ⁴Department of Neurology, Northwestern University, Feinberg School of Medicine, Chicago, IL; ⁵Department of Pediatrics, University Medical Center Hamburg-Eppendorf, Hamburg, Germany; ⁶Institute of Human Genetics, Helmholtz Center Munich, Neuherberg, Germany; ⁷Institute of Human Genetics, Technical University Munich, Munich, Germany; ⁸Maine Medical Partners Pediatric Specialty Care, Portland, ME; Department of Neurology, Boston Children's Hospital, Boston, MA; ¹⁰Department of Pathology, McGill University, Montreal Neurological Institute, Montreal, Canada; ¹¹Molecular Neurogenetics Unit, Institute for Research and Health Care (IRCCS) Foundation Carlo Besta Neurological Institute, Milan, Italy; ¹²GeneDx, Gaithersburg, MD; ¹³Kadlec Clinic Genetic Counseling, Richland, WA; ¹⁴Division of Genetic Medicine, Department of Pediatrics, Seattle Children's Hospital and University of Washington, Seattle, WA; 15Department of Pediatrics, Saint Justine University Hospital Center and University of Montreal, Montreal, Canada; and ¹⁶Montreal Neurological Institute, Department of Neurology and Neurosurgery, McGill University, Montreal, Canada

Address correspondence to Dr Campeau, Department of Pediatrics, Saint Justine Hospital, University of Montreal, Medical Genetics Service, Room 6727, 3175 Cote-Sainte-Catherine, Montreal, QC H3T 1C5, Canada. E-mail: p.campeau@umontreal.ca

Additional supporting information can be found in the online version of this article.

Received Nov 10, 2017, and in revised form Mar 6, 2018. Accepted for publication Mar 7, 2018.

View this article online at wileyonlinelibrary.com. DOI: 10.1002/ana.

ANNALS of Neurology

defects in VPS13A lead to the neurodegenerative disorder choreoacanthocytosis (Online Mendelian Inheritance in Man database [OMIM] 200150),⁵ whereas mutations of VPS13B and VPS13C cause Cohen syndrome (OMIM 216550)⁶ and autosomal recessive early onset Parkinson disease (OMIM 616840), respectively.⁷ Until now, VPS13D had not been associated with any human disease.

Subjects and Methods

This study was approved by local institutional review boards of all participating centers, and informed consent was obtained from all subjects or their parents when applicable. Clinical details were obtained through medical file review and direct examination. Genomic DNA was extracted from peripheral blood samples. Whole exome sequencing (WES) was performed on Family 1 using SureSelect Exon Capture v4 (Agilent, Santa Clara, CA) and paired-end sequencing on a HiSeq2500 (Illumina, San Diego, CA). Details on exome capture, sequencing, and analysis can be found in Gauthier et al.8 We identified rare variants (minor allele frequency [MAF] < 0.005) shared between individuals III-3 and III-4. Other families were recruited through GeneMatcher (https://genematcher.org/). In Family 2, trio WES and then Sanger sequencing-based segregation analysis including DNA sample of an unaffected sister, were performed as described before. 9,10 For Family 4, a quartetbased WES study failed to detect cosegregating biallelic mutations. WES was then performed in all 4 family members. Sample libraries were prepared using the Illumina Truseq PCR-free kit with paired-end sequencing preformed on a HiSeq X10 instrument. Bioinformatic analysis was performed as previously described.¹¹ Analysis initially focused on coding and splice-site biallelic variants with a MAF < 0.01 in ExAC, cg69, and 1000 Genomes Project. For Families 3 and 5, trio WES was performed as described previously, 12 and candidate gene selection was done using assertion criteria publicly available on the GeneDx ClinVar submission page (http://www.ncbi.nlm.nih.gov/ clinvar/submitters/26957/). Sanger sequencing was performed to confirm and validate cosegregation status of the candidate variants. SIFT,13 Polyphen-2,14 Mutation Taster,15 and Combined Annotation Dependent Depletion $(CADD)^{16}$ were the in silico tools used for pathogenicity predictions.

Results

Identification of the VPS13D Variants

Biallelic *VPS13D* variants were independently identified as the primary candidate genetic cause for dystonia in the 5 families reported herein (Table and Supplementary Table). Family 1 included 2 affected siblings who presented with childhood onset chorea and dystonia followed by slowly progressive spastic ataxia and mild intellectual disability. Extensive investigations performed prior to WES included genetic testing (Friedreich ataxia, autosomal recessive spastic ataxia of Charlevoix–Saguenay,

fragile X syndrome, array comparative genomic hybridization), vitamin E levels, and metabolic testing (fasting blood lactate, pyruvate and ketone bodies, plasma amino acids, urine organic acids), which were negative. Muscle biopsy of Individual III-3 showed subsarcolemmal mitochondrial aggregates with otherwise normal mitochondrial morphology, and mild lipidosis, which can both be markers of mitochondrial diseases. Given abnormal magnetic resonance imaging (MRI) findings in basal ganglia (detailed below) and muscle biopsy findings, respiratory chain as well as pyruvate dehydrogenase, pyruvate carboxylase, and glutaryl-CoA dehydrogenase enzymatic assays in fibroblasts were performed and were normal. We then performed WES (separate mitochondrial DNA sequencing was planned if the WES was negative) and compared all rare variants detected in both affected siblings. Among those, we identified 2 variants of interest (c.7332_7333del and c.10562A>G) in VPS13D. No pathogenic or likely pathogenic variants in known disease genes that would explain the phenotype of the patients were identified. Both VPS13D variants are novel and not present in the gnomAD database (http://gnomad.broadinstitute.org/) or previously described in the literature. Parental testing by Sanger sequencing confirmed the recessive mode of inheritance (biallelic; Fig 1A). Regarding the missense mutation, the substitution occurs at a residue that is highly conserved across species (see Fig 1C). Multiple in silico analyses predict this variant is damaging to the protein structure/function.

Through GeneMatcher and our network of collaborators, we identified 5 additional cases, with clinical phenotypes partially overlapping that of Family 1, from 4 unrelated families who underwent either WES (Families 2, 3, and 5) or whole genome sequencing (Family 4) and were found to also harbor rare likely pathogenic recessive variants in VPS13D (see Fig 1). After filtering, VPS13D was the best candidate gene identified in all families. Families 1, 3, and 4 have biallelic VPS13D variants affecting conserved residues and combining a missense mutation with a CADD score >19.5 and a loss-of-function mutation (see Fig 1). Family 2 is a consanguineous family, and the patient has a homozygous missense mutation, whereas the patient from Family 5 harbors compound heterozygous missense mutations. No other pertinent biallelic rare coding or de novo coding variants were detected in these families.

Clinical Features

All the patients with recessive *VPS13D* mutations presented with a slowly progressive childhood neurological disorder with an onset before 12 years of age. Common clinical features at presentation in 4 of the 5 families include global developmental delay, axial hypotonia, and

2 Volume 00, No. 00

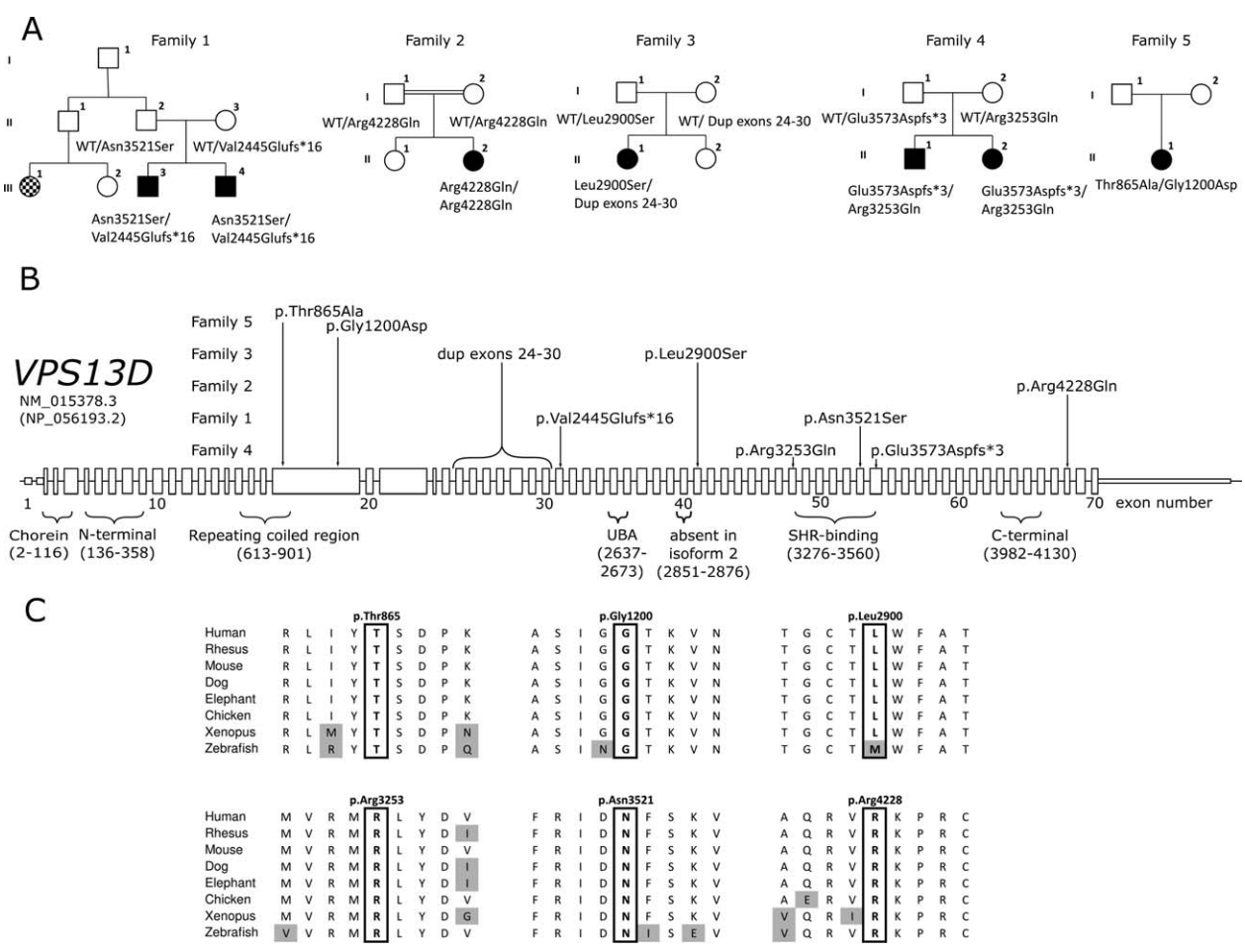


FIGURE 1: (A) Pedigrees of the families with VPS13D mutations. The solid symbols represent the movement disorder. The checkered symbol represents childhood onset epilepsy and learning disability. In Family 5, both mother and child have Schmidtype metaphyseal dysplasia. (B) Location of the mutations on the VPS13D gene, in order of age of onset of the disease (earliest on top). Introns are not drawn to scale. The labels under the gene refer to the domains and their amino acid positions, as compiled in Pfam (http://pfam.xfam.org). "Chorein" refers to the N-terminal region of chorein or VPS13 domain and is proposed to contain a leucine zipper. N-terminal and C-terminal refer to the VPS13 family N-terminal or C-terminal domains, UBA to the UBA protein domain, and SHR-binding to the SHR-binding domain of VPS13. The repeating coiled region domain of all VPS13 proteins includes a well-conserved P-x4-P-x13-17-G sequence.² (C) Conservation in vertebrates of the residues affected by missense mutations.

early onset chorea and mild intellectual disability, with development of progressive spastic ataxia and dystonia (focal or generalized) in adulthood (see Table and Supplementary Table). In contrast, patients from Family 4 had normal motor and cognitive development, and both subjects presented during childhood with a mild, non-progressive rest and action tremor in the upper limbs with progression to dystonia (cervical and brachial dystonia in Patient II:2 and brachial dystonia in Patient II:1 of Family 4) and pyramidal signs in the lower limbs in early adulthood; Patient II:2 has recently developed an overt progressive spastic paraparesis and mild cerebellar signs in the upper limbs.

Two patients (Family 3, Patient II-1 and Family 5, Patient II-1) have epilepsy. The most severe phenotype was seen in a child with symptom onset at 6 months of

age who has microcephaly, generalized dystonia, and chorea leading to an inability to ambulate at age 3 years (Family 3, Patient II-1). Microcephaly is present in 2 individuals with early onset disease (Family 3, Patient II-1; Family 5, Patient II-1).

MRI of the brain showed bilateral and symmetric putaminal and caudate T2/fluid-attenuated inversion recovery (FLAIR) hyperintensities accompanied by mild putaminal atrophy in 4 cases from 3 families (Fig 2, Supplementary Table). This MRI pattern led to an initial presumptive diagnosis of Leigh syndrome (OMIM 256000) in 2 families. Interestingly, the MRI pattern in Family 4 showed diffuse and extensive T2/FLAIR hyperintensities of the subcortical and periventricular white matter, the cerebellar peduncles, the posterior limb of the internal capsule, and to a lesser degree the corpus

Month 2018 3

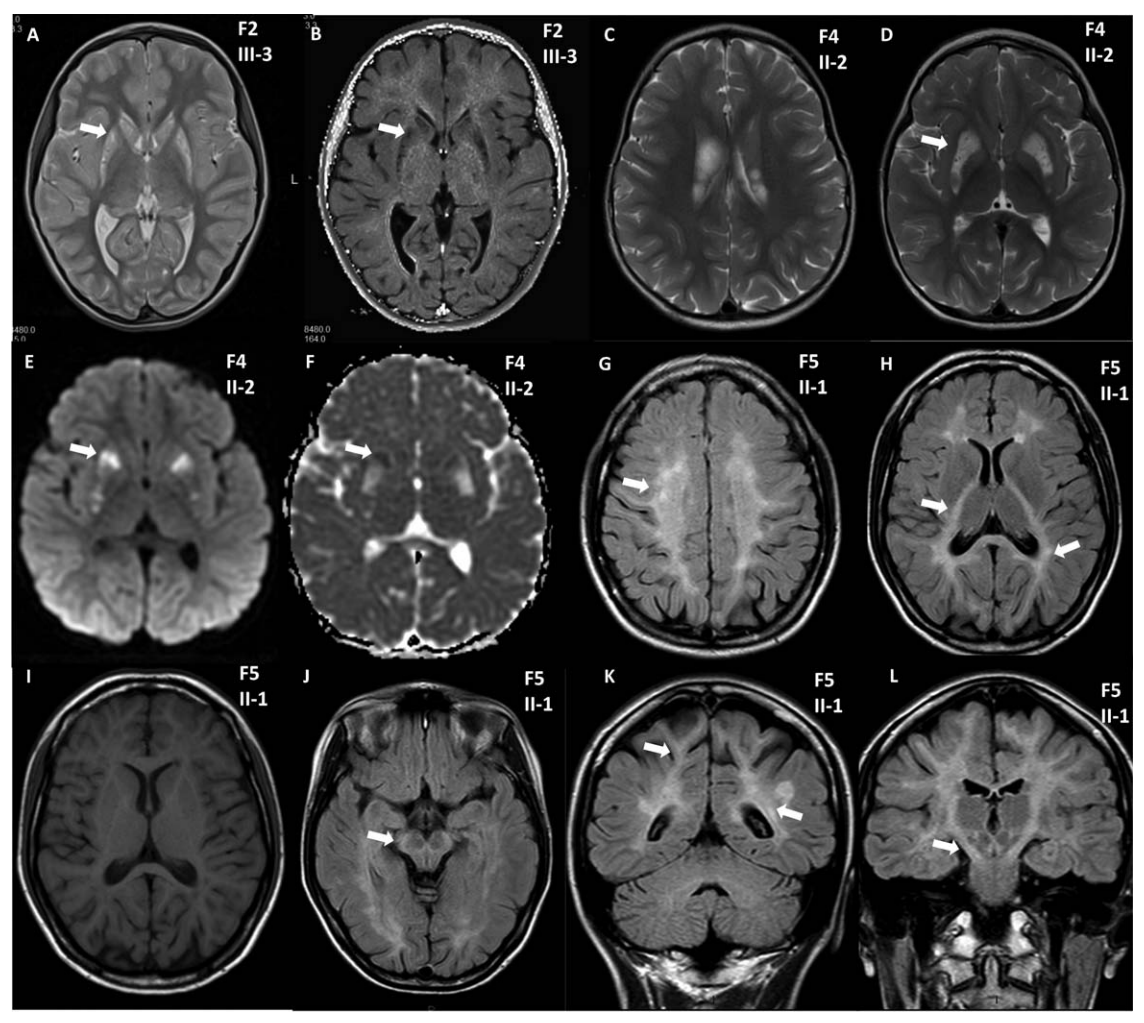


FIGURE 2: (A, B) Axial brain magnetic resonance imaging (MRI) from the proband of Family 2, II-2, showing homogenous, bilateral T2 hyperintensities (A) and correlating T1 hypointensities (B) in the caudate and putamen. (C-F) Axial brain MRI from proband of Family 3, II-1, showing homogenous, bilateral T2 hyperintensities in the caudate (C) and in the putamen (D) as well as patchy putaminal diffusion restriction demonstrated by diffusion-weighted imaging (E) and apparent diffusion coefficient (F) sequences. (G-L) Axial brain MRI from proband of Family 4, II-2, showing diffuse, bilateral T2 hyperintensities in the subcortical white matter (G), posterior limb of the internal capsule, and periventricular areas (H). The axial T1 image is normal (I). MRI also shows T2 hyperintensities of the cerebellar peduncles (J, L). Coronal view is shown of the posterior subcortical and periventricular T2 hyperintensities (K) as well as the peduncles (L).

callosum. MRI from the proband of Family 5 showed diffuse white matter atrophy. Individual II-2 from Family 2 and Individual II-2 from Family 4 had unchanged brain MRIs over 4 years.

Discussion

We provide clinical and genetic evidence supporting VPS13D mutations as a cause of a progressive childhood onset neurological disorder characterized in most cases by developmental delay, axial hypotonia, and hyperkinetic movement disorders associated with spastic paraparesis, as well as truncal and appendicular ataxia. The striking brain MRI findings are wide-ranging and include symmetrical caudate and putaminal hyperintense T2/ FLAIR signal or multifocal, widespread subcortical white matter

involvement with a hypointense T2 signal in the basal ganglia and putaminal atrophy (see Fig 2). The characteristics of the first MRI resemble Leigh syndrome MRI presentations, which consist of symmetrical T2 hyperintensities affecting the putamina, caudate heads, globus pallidus, thalamus, subthalamic nucleus, and brainstem (periaqueductal gray matter, pons, medulla); more rarely there is multifocal white matter involvement. ¹⁷ Interestingly, 3 patients in our cohort initially received a presumptive diagnosis of Leigh syndrome because of their imaging and clinical presentation, although the absence of sudden clinical deterioration, slow progression, and normal serum lactate levels did not support this diagnosis. Individual II-2 from Family 2 did have elevated cerebrospinal fluid lactate. The *VPS13D* clinical entity

4 Volume 00, No. 00

Family	1	1	2	3	4	4	5
ndividual, ender	III-3, M	III-4, M	II-2, F	II-1, F	II-1, M	II-2, F	II-1, F
Origin	French Canadian	French Canadian	Egyptian	European	Italian	Italian	Mixed ^a
VPS13D variants in NM_015378.3	c.7332_7333del (p.Val2445 Glufs*16); c.10562A>G (p.Asn3521Ser) (CADD = 27.1)	c.7332_7333del (p.Val2445 Glufs*16); c.10562A>G (p.Asn3521Ser) (CADD = 27.1)	c.12683G>A, p.Arg4228Gln (CADD = 35) homozygous	c.5853-94_7148 + 210dup; c.8699 T>C (p.Leu 2900Ser) (CADD = 28.6)	c.10694_10718dup, (p.Glu3573 Aspfs*3); c.9758G>A (p.Arg3253Gln) (CADD = 33)	c.10694_10718dup, (p.Glu3573 Aspfs*3); c.9758G>A (p.Arg3253Gln) (CADD = 33)	c.2593A>G, (p.Thr865Ala) (CADD = 24.2); c.3599G>A (p.Gly1200Asp) (CADD = 19.5)
Age at first symptoms	2 yr	4–5 y	1–2 yr	6 mo	12 yr	6–7 yr	Birth
Age at last evaluation	31 yr	33 yr	9 yr	3 yr	31 yr	29 yr	22 mo
Presenting symptoms	Gait instability, chorea, dysarthria	Gait instability, frequent falls	Gait instability	Developmental delay, torticollis	Upper limb tremor	Upper limb tremor	Hypotonia, GDD
Clinical diagnoses	Spastic ataxia with mild ID	Spastic ataxia with mild ID	Ataxia, muscle weakness, dystonia, mild ID	Generalized dystonia and chorea, GDD	Mild UL tremor and LL pyramidal signs	Spastic paraparesis and dystonia	Hypotonia, microcephaly, ataxia, GDD
Global development	Mild ID, learning disability	Mild ID	Motor delay and mild ID	GDD	Normal	Normal	GDD
Reflexes	Brisk (LL)	Brisk (LL)	Normal	Normal	Brisk (LL)	Brisk (LL)	N/A
Babinski	+	+	_	_	+	+	N/A
Ataxia	+	+	+	N/A	_	+	+
Chorea	+	-	+	+	_	-	+
Dystonia	+	_	_	+	+	+	+
Gait	Spastic ataxic	Spastic ataxic	Ataxic	Nonambulant	Normal	Scissoring	Spastic ataxic

^aItalian, Welsh, Irish, Yugoslavian, African American.

CADD = Combined Annotation Dependent Depletion-Phred score (not applicable to loss-of-function mutations); F = female; GDD = global developmental delay; ID = intellectual disability; LL = lower limb; M = male; N/A = not available; UL = upper limb.

should therefore be considered in the differential diagnosis of atypical Leigh syndrome cases without a molecular diagnosis as well as in cases with spastic paraparesis, spastic ataxia, and generalized dystonia with T2 hyperintensities in the basal ganglia and/or white matter on MRI. The VPS13D clinical spectrum in our cohort includes corticospinal tract dysfunction, cerebellar and extrapyramidal signs, hearing loss, and seizures together with bilateral symmetric T2 hyperintensities in the basal ganglia and/or brainstem suggestive of Leigh syndrome. Mitochondrial leukodystrophies also display a pattern of diffuse asymmetrical subcortical white matter and bilateral basal ganglia involvement. The VPS13D clinical spectrum suggests mitochondrial dysfunction as a

possible pathophysiological mechanism for this new clinical entity.

VPS13D is a member of the VPS13 family, which includes VPS13A. VPS13A mutations cause a neurodegenerative condition, choreoacanthocytosis, which presents with chorea associated with other movement disorders, cognitive decline, seizures, and elevated serum creatine kinase. Brain MRI in VPS13A biallelic mutation carriers typically reveals atrophy of the head of the caudate nuclei and putamina, which are hyperintense in T2, isointense in T1, and occasionally demonstrate susceptibility-weighted imaging–positive iron deposition. A few adults with VPS13A mutations have been reported with widespread areas of increased T2 signal in the cerebral white matter in

Month 2018 5

addition to the involvement of the basal ganglia, thalamus, cerebral peduncles, pons, and corpus callosum.²¹ This wide-ranging MRI pattern closely resembles the MRI findings from the patients with *VPS13D* mutations reported herein, suggesting a pathophysiological association.

There are multiple lines of genetic evidence for VPS13D being implicated in our observed phenotypes. The VPS13D contains 69 coding exons encoding 4,388 amino acids. Interestingly, although large, constraint metrics calculations in ExAC demonstrated that VPS13D is intolerant to variations.²² The Z score for missense variations in this gene is 1.85, meaning that VPS13D had fewer variants than expected. Moreover, VPS13D is extremely intolerant of loss-of-function (LoF) variations, with a pLi = 1.23 Although 103 LoF variations in VPS13D are reported in the gnomAD browser (>138,000 unrelated individuals), none of these was found in the homozygous state, reinforcing the low tolerance for this type of mutation in VPS13D. Interestingly, 3 of 5 families reported herein harbor an LoF variation, including Individual II-2 from Family 3, with a partial gene duplication of exons 24 to 30. This individual has the most severe phenotype in our cohort and is nonambulant because of generalized dystonia. Two of our 5 families have > 1 affected individual with biallelic variants in VPS13D.

Yeast Vps13p (homologue of human VPS13A) has a role in mitochondrial stability and possibly impedes mitochondrial autophagy.¹⁸ Recently, Vps13D was shown to play a role in mitochondrial fission, clearance, and autophagy (mitophagy) in Drosophila, and its knockout in human HeLa cells led to enlarged mitochondria.⁴ Based on pairwise comparisons between VPS13 gene family members and yeast Vps13p, Velayos-Baeza et al have identified the UBA domain (amino acid 2637-2673), which confers target specificity to multiple enzymes of the ubiquitination system.² This domain is absent from other VPS13 proteins, and Anding et al have shown that this domain is in part responsible for the ability of VPS13D to regulate mitochondrial size. 4 We did find some indications of mitochondrial alterations in muscle biopsy but found normal enzymatic activities in fibroblast cell lines. Anding et al have also identified Atg8-interacting motifs in Drosophila Vps13D, and have colocalized Vps13D with the lysosomal marker LAMP1. In addition, a predicted ricin-B-lectin motif (or SHR-binding domain), predicted to bind carbohydrates, is present in all VPS13 proteins including VPS13D.² The presence of this domain suggests that VPS13D might also interact with or be involved in trafficking of carbohydrates or carbohydrate-containing proteins.²

Roles identified in other VPS13 proteins are diverse.³ VPS13A is important for the cytoskeleton, vesicular

transport, autophagy, and the metabolism of phosphoinositides. VPS13B is important for maintenance of the Golgi morphology, adipogenesis, and protein glycosylation. VPS13C is present on mitochondria, lipid droplets, and early endosomes, and is involved in mitochondrial integrity and adipogenesis. Lesage et al found that loss of function mutations in *VPS13C* cause early onset parkinsonism by disrupting mitochondrial maintenance. Its knockdown causes perinuclear redistribution of mitochondria, mitochondrial fragmentation, decreased mitochondrial transmembrane potential, and increased PINK1- and parkinmediated mitophagy.⁷

The identified missense variants do not cluster in a particular region of this gene, and this, along with the finding that the missense variants are often found in *trans* with loss-of-function mutations, suggests that these missense variants are also likely to cause loss/reduction of function. Disorders associated with the 3 other members of the VPS13 family are all recessive, present some phenotypic overlap with our families, and include missense and truncating mutations (OMIM 200150, 216550, 616840). Thus, the phenotypic spectrum and radiological pattern presented here, in addition to previously reported functional studies in yeast and *Drosophila*, suggest mitochondrial dysfunction in *VPS13D*-related movement disorder pathophysiology.

Acknowledgment

This study was supported by the German Bundesministerium für Bildung und Forschung through the E-Rare project GENOMIT (01GM1603, H.P.) and by EU Horizon2020 Collaborative Research Project SOUND (633974, H.P.).

We thank all patients and families.

Author Contributions

J.G. and P.M.C. contributed to the conception and design of the study. All authors contributed to the acquisition and analysis of data. J.G., I.A.M., and P.M.C. contributed to drafting the text or preparing the figures.

Potential Conflicts of Interest

A.T. and L.B.H. are employees of GeneDx, a wholly owned subsidiary of OPKO Health. GeneDx provides genetic testing services that might be used to diagnose this condition. The other authors have nothing to report.

References

- Fahn S, Jankovic J, Hallett M. Principles and practice of movement disorders. 2nd ed. Edinburgh, UK; New York, NY: Elsevier/ Saunders, 2011.
- Velayos-Baeza A, Vettori A, Copley RR, et al. Analysis of the human VPS13 gene family. Genomics 2004;84:536–549.

6 Volume 00, No. 00

- Rzepnikowska W, Flis K, Munoz-Braceras S, et al. Yeast and other lower eukaryotic organisms for studies of Vps13 proteins in health and disease. Traffic 2017;18:711–719.
- Anding AL, Wang C, Chang TK, et al. Vps13D encodes a ubiquitinbinding protein that is required for the regulation of mitochondrial size and clearance. Curr Biol 2018;28:287.
- Rampoldi L, Dobson-Stone C, Rubio JP, et al. A conserved sorting-associated protein is mutant in chorea-acanthocytosis. Nat Genet 2001;28:119–120.
- Kolehmainen J, Black GC, Saarinen A, et al. Cohen syndrome is caused by mutations in a novel gene, COH1, encoding a transmembrane protein with a presumed role in vesicle-mediated sorting and intracellular protein transport. Am J Hum Genet 2003;72: 1359–1369
- Lesage S, Drouet V, Majounie E, et al. Loss of VPS13C function in autosomal-recessive parkinsonism causes mitochondrial dysfunction and increases PINK1/parkin-dependent mitophagy. Am J Hum Genet 2016;98:500–513.
- Gauthier J, Ouled Amar Bencheikh B, Hamdan FF, et al. A homozygous loss-of-function variant in MYH11 in a case with megacystis-microcolon-intestinal hypoperistalsis syndrome. Eur J Hum Genet 2015;23:1266–1268.
- Hempel M, Casar Tena T, Diehl T, et al. Compound heterozygous GATA5 mutations in a girl with hydrops fetalis, congenital heart defects and genital anomalies. Hum Genet 2017;136:339–346.
- Kremer LS, Bader DM, Mertes C, et al. Genetic diagnosis of Mendelian disorders via RNA sequencing. Nat Commun 2017;8:15824.
- Mencacci NE, Kamsteeg EJ, Nakashima K, et al. De novo mutations in PDE10A cause childhood-onset chorea with bilateral striatal lesions. Am J Hum Genet 2016;98:763–771.
- Tanaka AJ, Cho MT, Millan F, et al. Mutations in SPATA5 are associated with microcephaly, intellectual disability, seizures, and hearing loss. Am J Hum Genet 2015;97:457–464.

- Kumar P, Henikoff S, Ng PC. Predicting the effects of coding nonsynonymous variants on protein function using the SIFT algorithm. Nat Protoc 2009;4:1073–1081.
- Adzhubei IA, Schmidt S, Peshkin L, et al. A method and server for predicting damaging missense mutations. Nat Methods 2010;7: 248–249.
- Schwarz JM, Cooper DN, Schuelke M, Seelow D. MutationTaster2: mutation prediction for the deep-sequencing age. Nat Methods 2014;11:361–362.
- Kircher M, Witten DM, Jain P, et al. A general framework for estimating the relative pathogenicity of human genetic variants. Nat Genet 2014;46:310–315.
- Bonfante E, Koenig MK, Adejumo RB, et al. The neuroimaging of Leigh syndrome: case series and review of the literature. Pediatr Radiol 2016;46:443–451.
- Park JS, Thorsness MK, Policastro R, et al. Yeast Vps13 promotes mitochondrial function and is localized at membrane contact sites. Mol Biol Cell 2016;27:2435–2449.
- Walker RH, Jung HH, Dobson-Stone C, et al. Neurologic phenotypes associated with acanthocytosis. Neurology 2007;68: 92–98
- Lee JH, Lee SM, Baik SK. Demonstration of striatopallidal iron deposition in chorea-acanthocytosis by susceptibility-weighted imaging. J Neurol 2011;258:321–322.
- Nicholl DJ, Sutton I, Dotti MT, et al. White matter abnormalities on MRI in neuroacanthocytosis. J Neurol Neurosurg Psychiatry 2004;75:1200–1201.
- Karczewski KJ, Weisburd B, Thomas B, et al. The ExAC browser: displaying reference data information from over 60 000 exomes. Nucleic Acids Res 2017;45(D1):D840–D845.
- 23. Lek M, Karczewski KJ, Minikel EV, et al. Analysis of protein-coding genetic variation in 60,706 humans. Nature 2016;536:285–291.

Month 2018 7